The Journal of Neuroscience, May 1994, 14(5): 3166–3179

bendless, a *Drosophila* Gene Affecting Neuronal Connectivity, Encodes a Ubiquitin-conjugating Enzyme Homolog

Charles Euk Oh,[1] Ross McMahon,[2] Seymour Benzer,[3] and Mark A. Tanouye[1]

[1]Department of Entomology and Parasitology, University of California at Berkeley, Berkeley, California 94720, [2]Beckman Research Institute, City of Hope, Duarte, California 91010, and [3]Division of Biology, California Institute of Technology, Pasadena, California 91125

The *Drosophila bendless* (*ben*) gene was originally isolated as a mutation affecting the escape jump response. This behavioral defect was ascribed to a single lesion affecting the connectivity between the giant fiber and the tergotrochanter motor neuron. A closer examination of the *ben* phenotype suggests that *ben* activity is broader and affects a variety of other neurons including photoreceptor cells and their axons. Mosaic analysis indicates that the focus of *ben* activity is presynaptic. We have cloned the *ben* gene through a chromosomal walk and show that it is homologous to a class of ubiquitin-conjugating enzymes. The major role of ubiquitination in the protein degradative pathway suggests that *ben* regulates neural developmental processes such as growth cone guidance by targeting specific proteins for degradation.

***[Key words: axon pathfinding, neural connectivity, escape response, giant fiber system, ubiquitin-conjugating enzyme,* Drosophila bendless]**

The development of nervous systems requires that neurons extend axons over long distances through diverse environments. Remarkable specificity is displayed in the way axons navigate to their specific targets, and by the stereotypic patterns of projections and connections reproduced in each organism.

Fidelity in nervous system development is achieved through a multitude of mechanisms. Growth cones of developing neurons make a stepwise series of pathway choices based on cell-to-cell and cell-to-substrate interactions (Caudy and Bentley, 1986; Bovolenta and Dodd, 1990; O'Rourke and Fraser, 1990). These interactions involve both adhesive and repulsive molecules that label particular axon pathways and serve as critical recognition markers for the developing growth cone (Dodd and Jessell, 1988; Keynes and Cook, 1990; Hynes and Lander, 1992). Thus, axons can navigate by selective recognition and adhesion to or repulsion from such labeled pathways (Cox et al., 1990; Jay and Keshishian, 1990; Grenningloh et al., 1991). In other cases, gradients of chemotropic factors secreted by the targets appear to function as a guidance mechanism (Tessier-Lavigne et al., 1988; Okamato and Kuwada, 1991; Tessier-Lavigne, 1992). Thus, neurons use various external guidance cues to navigate to their targets.

Whatever constitutes the set of guidance cues, the developing growth cone must recognize these signals, and through some signal transduction mechanism, mount appropriate physiological responses (Kater and Guthrie, 1990; Lohof et al., 1992). The growth cone therefore represents a dynamic cellular structure that constantly translates changing environmental cues into structural and functional transformations. These transformations include the continuous assembly and disassembly of cytoskeletal elements, and the turnover of old and expression of new cell surface components (Dodd et al., 1988; Smith, 1988; Tanaka and Kirschner, 1991). Therefore, not only are external cues important for axon guidance, but also the ways in which the developing growth cone perceives the cues play a critical role in guiding the axon. This complex web of interactions must require layers of regulatory mechanisms to generate a properly connected nervous system.

To help understand this intricate biological process, mutations affecting development of the patterns of neuronal circuitry have been employed (Bovolenta and Dodd, 1991; Gao et al., 1992; McIntire et al., 1992). The ease of genetic manipulation in *Drosophila melanogaster* has allowed systematic searches for genes whose mutations specifically disrupt defined neural elements (Bier et al., 1989; Seeger et al., 1993). This has allowed the characterization of a number of molecules that appear important for pathfinding and connectivity in the fly nervous system (Grenningloh et al., 1990, 1991; Nose et al., 1992; Krishnan et al., 1993).

One neural circuit that has been a target of such analysis is the giant fiber (GF) system mediating the escape jump response. It is a relatively simple neural circuit that has been defined both morphologically and electrophysiologically (King and Wyman, 1980; Tanouye and Wyman, 1980; King and Tanouye, 1983; Koto, 1983; Trimarchi and Schneiderman, 1993). The GF is a command neuron that receives input from the visual and olfactory centers, and upon stimulation, drives the tergotrochanteral (TTM), dorsal longitudinal (DLM), and dorsoventral muscles (DVM) (see Fig. 1*A* for details). A mutagenesis screen for genes disrupting this circuit led to the identification of a gene, *bendless* (*ben*), that affects a single neuronal connection between

Received June 24, 1993; revised Oct. 22, 1993; accepted Nov. 1, 1993.

We thank Drs. William Trevarrow and Ken McCormack for contributions to aspects of this work. We are grateful for technical assistance from Rommel Valero, Kawanaa Areceneaux, and Rosalind Young, and the management of fly stocks by Sally Faulhaber. We thank Drs. Mani Ramaswami, Elaine Reynolds, Jeremy Lee, and Paul Pavlidis for critical reading of the manuscript. This research was supported by a fellowship from the Jane Coffin Childs Memorial Fund for Medical Research and an NIH postdoctoral fellowship to C.E.O., NSF Grant BNS 9120084 to M.A.T., and grants to S.B. from the NSF (BC58908154), the NIH (EY09278), and the James G. Boswell Foundation.

Correspondence should be addressed to Charles Oh, 201 Wellman Hall, University of California at Berkeley, Berkeley, CA 94720.

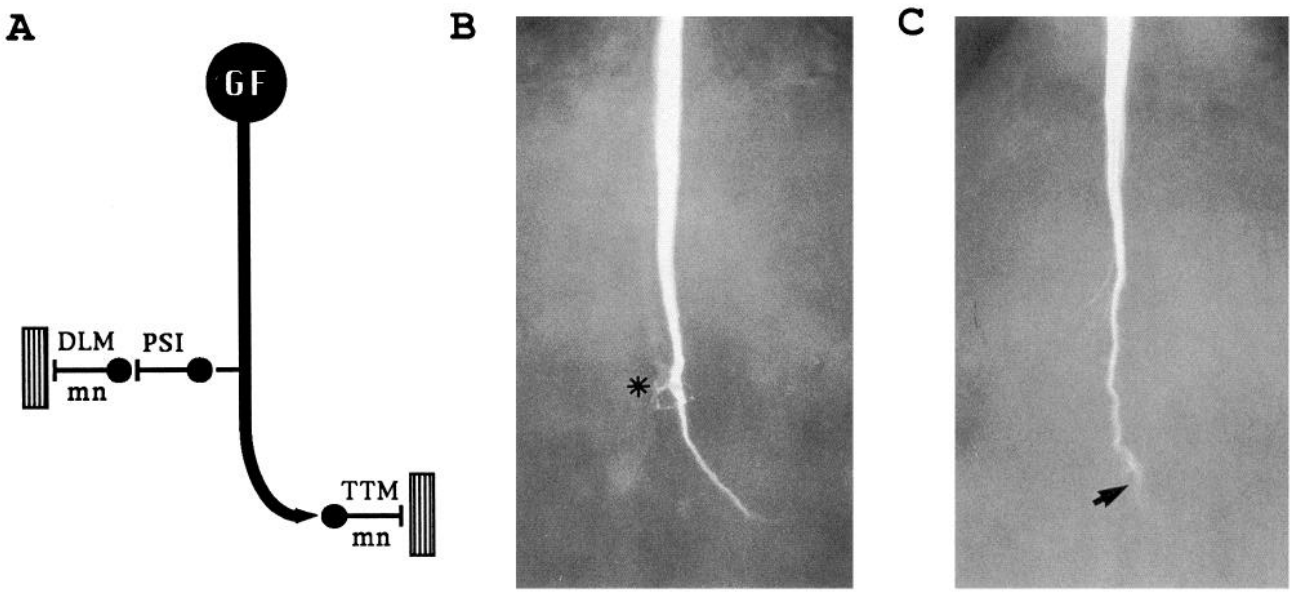

Figure 1. *A*, Schematic representation of the cellular elements of the *Drosophila* giant fiber system. The giant fibers (*GF*) are command interneurons that drive an escape jump. The diagram shows elements of one hemisegment. The two GF cell bodies and their dendrites are in either side of the brain and receive synaptic inputs from the visual and antennal centers. The GF outputs are in the thoracic ganglion. One is to the contralateral dorsal longitudinal muscle (*DLM*) via a peripherally synapsing interneuron (*PSI*) and DLM motor neurons (*DLMmn*). After a terminal bend, the GF makes a second output to the ipsilateral tergotrochanter jump muscle (*TTM*) via the TTM motor neuron (*TTMmn*), which drives the escape jump. For simplicity, the five DLMmns and six DLM fibers are depicted as single elements. The GF also makes output pathways (not shown) to the three dorsoventral muscle (DVM I to DVM III) via multineuronal pathways; the cellular elements which define these pathways remain largely unidentified. The diagram summarizes the results of several studies (King and Wyman, 1980; Tanouye and Wyman, 1980; King and Tanouye, 1983; Tanouye and King, 1983). *B*, GF of wild-type CS flies. The morphology of the GF as revealed by injected Lucifer yellow dye shows an axonal projection that extends through the cervical connective and down the dorsal midline of the thoracic ganglion, terminating in the mesothoracic neuromere. In the neuromere, the GF synapses with the PSI in a tuft of short dendritic branches (*), and then turns laterally, making a connection to the TTMmn. *C*, GF of a *ben*^{1} mutant. The morphology of the GF in *ben*^{1} flies is normal in most respects as it courses through the thoracic ganglion. However, in the mesothoracic neuromere, while the *ben*^{1} GF connects to the PSI, it fails to complete the lateral bend and does not form its normal connection with the TTMmn dendrite. In many cases, fine irregular dendritic processes emanate from the terminus (*arrow*).

the GF and the TTM motor neuron (TTMmn) (Thomas and Wyman, 1982, 1984). Neuroanatomical studies using Lucifer yellow dye fills show that the GF in *ben* flies fails to extend a turn shortly before its connection with the TTMmn (Thomas and Wyman, 1982; Fig. 1*B,C*). The TTMmn itself is morphologically normal and terminates at the correct position in the mesothoracic neuromere (Koto, 1983). Electrophysiologically, the GF defect results in an increase in the latency and lability of the TTM response following GF stimulation. Remarkably, another output of the GF, the DLM, is unaffected in the mutant. Because of the narrow focus of its activity, the *ben* gene product was advanced as a candidate molecule affecting the formation of a single specific synapse.

We have examined *ben*^{1} flies to determine how the mutation influences axon guidance. From a combination of behavioral and anatomical analysis, we observed that *ben*^{1} affects neurons other than the GF such as photoreceptor cells and their axons. Like the *ben*^{1} GF, the photoreceptor axons initially project properly, but fail later in their pathway. Additional defects are seen in the organization of the rhabdomeres and the lamina. To determine how the lesions relate to the nature of the *ben* product, we conducted a molecular analysis of the gene. Surprisingly, *ben* is homologous to an enzyme that functions in the ubiquitination pathway. Because biochemical and genetic studies demonstrate that the ubiquitination pathway functions to target proteins for degradation, we suggest that *ben* functions to regulate neural development by targeting specific proteins for degradation. The presynaptic nature of the *ben*^{1} defect suggests new ways to consider how neural elements such as growth cones regulate their activity.

Materials and Methods

Fly strains. Chromosomes carrying the *ben*^{1} mutation and *Df(1)HA92* were obtained from Dr. J. Thomas (Salk Institute, San Diego, CA). The *ben*^{1} allele is an ethylmethanesulfonate-induced mutation described previously (Thomas and Wyman, 1984). The chromosomes carrying the R301.2 transposon insertion were obtained from Dr. A. Spradling (Carnegie Institute, Baltimore, MD). The deletion chromosomes *Df(1) ben*^{CO1} and *Df(1) ben*^{CO2} were generated by x-ray irradiation (4000 rad) of the R301.2 chromosome. About 50,000 mutagenized chromosomes were examined in a *ry*$^{-}$ background for loss of the R301.2 transposon, which is marked with *ry*$^{+}$. Deficiency and duplication chromosomes are described in the Figure 4 caption. All other mutations are described in Lindsley and Zimm (1992).

Mosaic analysis. For mosaic analysis, males of the genotype *y ben sd f* were crossed with *In(1)d149 y w lz/R(1)2In(1)w*^{vc} females. Gynandromorphs, arising from loss of the unstable ring X chromosome, were scored for head and thorax genotypes using external markers *y* and *f*. Only those flies showing extensive presence of the markers in the head or thorax were examined electrophysiologically for the *ben*^{1} phenotype. A total of six flies with markers exclusively in the head and seven flies with markers exclusively in the thorax were analyzed.

The distance between the anlage of two structures in the fly is represented by the Sturt, which is a 1% probability of a mosaic boundary occurring between the two structures at the blastoderm stage. The larger the value in Sturts, the greater the distance in the embryonic origins of the two structures (Hotta and Benzer, 1972). In our study, the fate map distance between the brain and thoracic ganglion is near the theoretical limit of 50 Sturts (Kankel and Hall, 1976). Thus, mosaic flies with mutant tissue exclusively in the head or in the thorax are easily generated. Examination of external markers should be sufficient in most

individuals to infer the genotype of the brain, which contains the cell body of the giant fiber neuron, since the fate map distance between the brain and the cuticle in the head is small, about 15 Sturts. The genotype of the mesothoracic neuromere is less well correlated with the thoracic cuticular phenotype (a separation of about 30 Sturts). Nevertheless, the focus of the *ben* defect can be determined from the head genotype alone. If the focus of the *ben* defect is in the giant fiber cell body, a *ben* phenotype will typically be observed when the head genotype is mutant, but not when the head genotype is wild type.

Photochoice and jump behavior analysis. A T-maze apparatus was used to test photochoice (Ballinger and Benzer, 1989). Flies were placed in a middle chamber that can be slid into position between two transparent plastic tubes, each illuminated from the end, one with green light, the other with UV. For each trial, 10–50 flies were light adapted under diffuse white light for 15 min, tested in the maze for 45 sec, and then counted. Flies were tested four to five times to obtain a quantitative phenotype. Photochoice ratios were determined from the total number of flies choosing UV or visible light. The number of flies observed are as follows (UV/visible): Canton-S (CS), 153/6; *ben*^{1}, 202/153; *sev*^{dc}, 9/82; *w m ben*^{1}, 47/9; *w m ben*^{1};P[w^+T65], 50/2; and *w m ben*^{1};P[w^+T25], 27/1. In the case of *w m ben*^{1}, the slight UV preference is actually due to a photophobic behavior. When given a choice between light and no light, *w m ben*^{1} choose dark:light at a 5:1 ratio, in contrast to CS flies, which choose dark:light at 1:7. The transgene *w m ben*^{1};P[w^+T65] is similar to CS in choosing dark:light at 1:11.5. The dark:light ratios were determined from examining the following number of flies (dark/light): *w m ben*^{1}, 51/10; CS, 12/85; *w m ben*^{1};P(w^+T65), 4/46. The slight photophobic behavior of *w m ben*^{1} flies is probably due to the absence of eye pigments.

To test jump behavior, flies were placed in an inverted round bottom flask or a clear plastic vial of 3 × 15 cm. A light-off stimulus of 20 or 60 msec duration from a fluorescent bulb was applied to the flies at 6 sec intervals. Flies were examined for 1 min. *ben*^{1} flies never mediate a jump response.

Electrophysiological analysis of the GF system. Electrophysiological analyses of *ben* defects were according to a modification of the method of Tanouye and Wyman (1980). In brief, individual flies were mounted on a glass slide using cyanoacrylate adhesive. Two uninsulated tungsten stimulating electrodes were inserted in the brain. Uninsulated tungsten recording electrodes were inserted into the tergotrochanter muscle (TTM) and the dorsal longitudinal muscle (DLM). Other insertions were as described in the text. In all cases, the muscles examined had insertions in the scutum that facilitated muscle identification. A tungsten electrode inserted into the abdomen served as ground. Electrical stimulus was a 3–5 V square pulse 0.2 msec in duration, usually delivered at 1.0 Hz from a Dagan S900 stimulator. A digital storage oscilloscope (Hitachi) was used to record responses. Latencies are measured from the end of the stimulus and the initiation of the evoked muscle response.

Determination of ben^1 *genotypes.* In many of the analyses reported here, *ben*^{1} genotypes were determined by both jump tests and by electrophysiology. Jump tests, although more convenient, were not completely reliable. Efficient jump tests generally required a *bw;st* background (Thomas and Wyman, 1984), which made analysis difficult in many cases due to the requirement for scoring *g* or *ry* phenotypes. Electrophysiological determinations were reliable, and all genotype identifications reported here are based on this method. Usually, genotype identifications were made by establishing strains and scoring at least five flies for electrophysiological response. As an example, for determining the *g–ben* interval by recombination, 158 separate recombinant lines were established and electrophysiological recordings were obtained from 533 flies. Similarly, 127 flies from 18 separate recombinant lines were examined electrophysiologically in mapping the *ben–na* intervals. Electrophysiological determinations of *ben* phenotypes were used in generating all multiply marked *ben* chromosomes, mapping *ben* with respect to one duplication and five deficiency chromosomes (see Fig. 4), testing recombinants in the RFLP analysis (see Fig. 6*A*), testing head–thorax genetic mosaics (Table 1), and testing for rescue in germline transformants (Table 2).

Examination of photoreceptors, photoreceoptor axons, and the giant fiber. Larval eye disk–brain preparations were examined with mAb 22C10, which stains nerve cells and axons (Zipursky et al., 1984). A fluorescein isothiocyanate (FITC)-conjugated anti-mouse antibody was used as the secondary antibody. Electron microscopic examinations of the retina and lamina were conducted as described (Ready et al., 1976).

The projection patterns of R7 and R8 axons were determined using a horseradish peroxidase (HRP) staining method (Benzer, 1991). A crystal of HRP was placed in the retina through a small slit, which was then sealed with vacuum grease to prevent desiccation. Following a 1 hr incubation, fly heads were embedded in OCT compound and sectioned (10 μm) by cryostat, and the HRP was visualized using diaminobenzidine and hydrogen peroxide. Sections containing the medulla optic lobe were examined under glycerol. Although the HRP is taken up by all photoreceptor cells, only the axons of photoreceptors R7 and R8 terminate in the medulla, where their projections can be readily seen.

Lucifer yellow dye fills of the GF were conducted according to Koto et al. (1981). Dye was injected iontophoretically with hyperpolarizing pulses of 5–100 nA; labeling of the GF was monitored by epifluorescence. Flies were fixed overnight in 4% formaldehyde-PBS and the thoracic ganglion dissected out. The ganglion was dehydrated in ethanol and cleared in methyl benzoate, and the GF was visualized by epifluorescence on a Zeiss Axiophot microscope. A minimum of four flies from each of three transformant lines [*w m ben*^{1}; P(w^+)] were examined along with Canton-S, *ben*^{1}, and *w m ben*^{1} flies.

Molecular biological techniques. Standard molecular biological methods were used as described (Sambrook et al., 1989). Lambda phage libraries were in EMBL3 vector with Canton-S and Oregon-R genomic DNA inserts. A cosmid genomic library in cosPer vector was provided by Dr. J. Tamkun (University of California at Santa Cruz). Embryonic (3–12 hr) and pupal cDNA libraries were in λgt10 vector (Poole et al., 1985). Also, an embryonic (0–24 hr) cDNA library prepared in λEXLX was provided by Dr. M. Strathman (University of California at Berkeley). All cDNAs were subcloned into pBluescript (Stratagene, La Jolla, CA) for subsequent analysis.

Complete DNA sequences of clones were generated from nested transposon insertions (Strathman et al., 1991; Gold Biotechnology, St. Louis, MI) using the Cycle Sequencing Kit (Bethesda Research Labs, Gaithersburg, MD). Sequences were assembled using the ASSEMBLYLIGN program (IBI, New Haven, CT). Data base searches were conducted using the FASTA program (Pearson and Lipman, 1988) and sequence analysis performed using MACVECTOR (IBI).

For Northern analysis, total RNA was isolated from various developmental stages by the RNazol-B method (Biotecx, Friendswood, TX). PolyA$^+$ RNA isolated using oligo-dT cellulose was fractionated on formaldehyde-agarose gels and transferred to nylon membranes. Filters were hybridized with DNA probes generated by a random primer labeling method.

RFLP analysis. Transheterozygous flies of the genotype *ben sd f/wy* R301.2;*ry*^{42} were used to obtain male recombinants between R301.2 and *ben*. From a screen of 12,000 F1 males, 32 +;*ry*^{42} lines were established. DNA was isolated from each line, digested with various restriction enzymes, and analyzed by Southern blotting. DNA from *ben sd f;ry*^{42} and *wy* R301.2; *ry*^{42} flies were used as controls. Labeled DNA probes were generated by random primer labeling (Stratagene) of whole genomic phage clones or isolated restriction fragments.

P-element transformation. An 18 kilobase (kb) genomic insert in λEMBL3 (λ8-10A) was excised by digestion with SalI and cloned into the XhoI site of CasPer4 (a gift of Linda Iverson, City of Hope, Duarte, CA). A 6 kb XhoI fragment contained in the same phage clone was also cloned into CasPer4. Constructs (1 mg/ml) were injected with phsπΔ2-3 helper plasmid (0.2 mg/ml) into w^{1118} embryos (Roberts, 1986). Eleven transformants were obtained for the 6 kb XhoI construct while five transformants were obtained for the 18 kb construct. To test for rescue, *w m ben*;P[w^+] males were generated from a cross of *w m ben/FM6* and transformant *w*;P[w^+] flies.

Results

Effects of ben^1 *mutation on the GF system*

In this report, we confirm previous electrophysiological observations that *ben*^{1} affects the escape jump (GF-TTM) pathway (Fig. 2). The *ben*^{1} GF drives the TTM at abnormally long latencies and the response fails completely at moderate frequencies of stimulation. In contrast, *ben*^{1} does not affect the stimulation of the wing depressor muscles (GF-DLM pathway): the mutant response has a normal latency and is capable of following high frequencies of stimulation. We have extended electrophysiological observations on the GF system to examine if three other GF outputs, to each of the three wing elevator DVM muscles are affected (Fig. 2). The DVM III response is unaltered

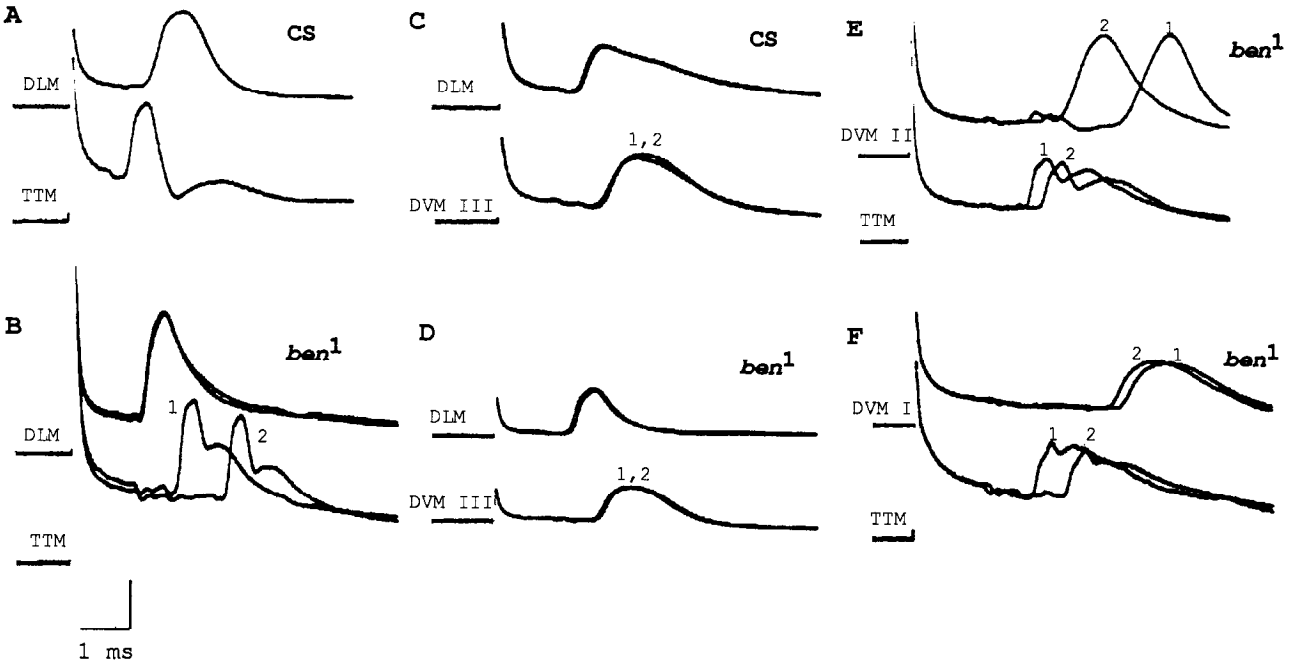

Figure 2. Electrophysiology of the GF system in wild-type (*CS*) and *ben*^{1} mutants. Recordings were made from various muscles following electrical activation of the GF (Tanouye and Wyman, 1980). The interval between successive recordings is 1 sec. *A*, Wild-type TTM and DLM responses. The latency of the GF-TTM response is very short, 0.96 ± 0.05 msec (mean ± SD). TTM potentials follow frequencies as high as 300 Hz for six stimuli (cf. Tanouye and Wyman, 1980). The latency of the GF-DLM response is somewhat longer, 1.54 ± 0.08 msec. DLM potentials follow frequencies as high as 100 Hz for nine stimuli. *B*, TTM and DLM recordings in a *ben*^{1} mutant. The GF-DLM pathway appears normal in *ben*^{1} mutants: the response has a short latency (1.45 ± 0.11 msec), and follows high-frequency stimulation. However, the *ben*^{1} GF drives the TTM abnormally: the latency is long and highly variable, and the response cannot follow even moderate frequencies of stimulation. A common observation seen in response to a 1.0 Hz stimulus is that the first stimulus delivered to the GF drives a long-latency response in the TTM (about 3 msec); subsequent stimuli drive successively longer-latency responses until no response is seen. Thus, although the *ben*^{1} TTM response will be identified here by the latency (mean ± SD = 2.67 ± 0.68 msec), it provides an incomplete picture of the abnormality. *C*, Wild-type DVM responses. The latency of the GF-DVM III response is 2.17 ± 0.16 msec. The DVM I and DVM II responses (not shown) are longer and more variable, 4.45 ± 1.06 and 4.47 ± 0.86 msec, respectively. *D*, DLM and DVM recordings in *ben*^{1} mutants. A DVM III response is shown: it has a normal latency (2.33 ± 0.18 msec) and no lability on a second stimulation. *E* and *F*, Comparison of TTM and DVM II/DVM I responses in *ben*^{1} mutants. It is difficult to be certain that the *ben*^{1} mutation has no effect on DVMI and DVMII because wild-type responses themselves show a considerable amount of variability. However, within the resolution of our measurements there is apparently no effect; the observed latencies of 4.08 ± 0.72 msec for DVM I and 5.29 ± 1.59 msec for DVM II are similar to wild-type values. In addition, although the *ben*^{1} TTM and DVM II responses have similar long and variable latencies, a close comparison of individual responses shows that they vary independently. In two successive recordings (*1* and *2*), the latency of TTM increases while that of DVM II decreases. The independence of the latencies suggest that different neuronal pathways are mediating the two responses. Similar results are observed in comparing *ben*^{1} TTM and DVM I responses (*F*). Vertical calibration is 10 mV for TTM traces and 20 mV for all others.

in *ben*^{1} flies: the latency of the response is normal and no lability in the signals is seen. The mutation also does not appear to alter DVM I and DVM II pathways. Although normal flies show in these pathways evoked potentials with considerable variation in latency (Tanouye and Wyman, 1980), *ben*^{1} flies show no additional variation or lability. Furthermore, the pathways for the DVM and TTM share a common element, the GF. A change in latency (or failure) of the TTM response due to a GF defect may result in coincident responses in DVM I and DVM II. In *ben*^{1} flies, changes in latency or failures of the TTM responses are not seen in the DVM I and DVM II responses. Thus, the pathways for all the DVMs appear unaffected by the *ben*^{1} mutation. The absence of identifiable electrophysiological changes in these other outputs support the view that, in the GF network, the defect is localized to the GF-TTM pathway.

General observations on ben^1 *mutants*

The *ben*^{1} mutation was isolated as a behavioral mutant thought to be specifically defective in escape jump (Thomas and Wyman, 1982). Flies carrying the *ben*^{1} mutation, however, show a number of general abnormalities. Recent evidence has indicated that *ben*^{1} mutants have abnormal grooming behavior (Phillis et al., 1993). The *ben*^{1} mutants also appear to be uncoordinated and lethargic: mutants remain at the bottom of the culture vial and do not show climbing behavior like normal flies. Mutants are capable of flying, but will not initiate flight when dropped from a height. Also, *ben*^{1} flies are less viable than normal flies. We observe that approximately 60% of the mutant pupae cannot successfully eclose and often die during emergence. The reduction in viability has been recently documented by Edgecomb et al. (1993).

Photochoice behavior and defects in the visual system

The general behavioral abnormalities of *ben*^{1} flies suggested the presence of other defects in the escape jump response. The light-off stimulus triggering the escape jump is perceived by the visual system, which in turn drives the GF. Therefore, along with defects in the GF-TTM pathway, abnormalities affecting the pathway from the visual center to the GF can also affect jump behavior. Here, we describe another major *ben*^{1} behavioral de-

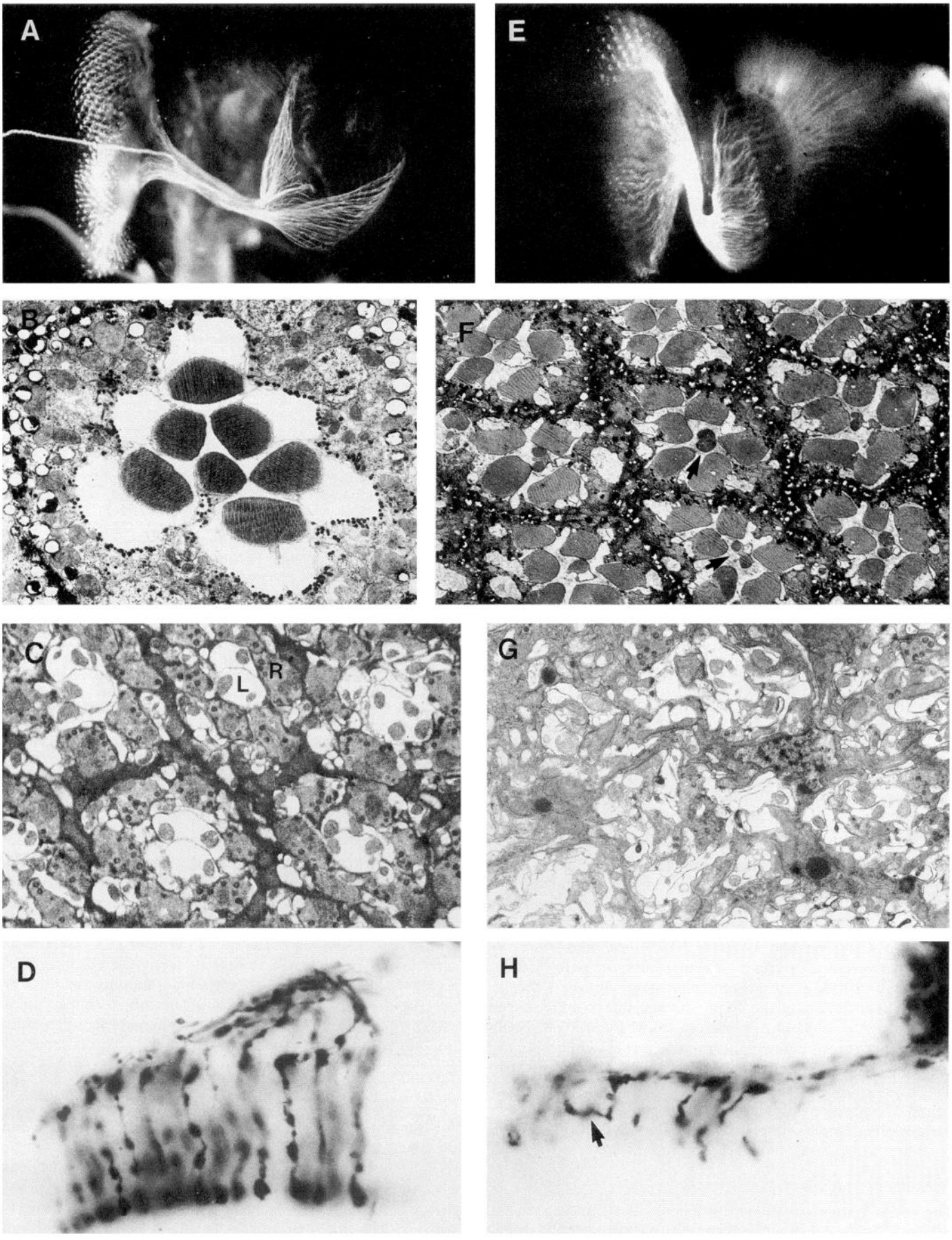
A
E
B
F
C
L
R
G
D
H

Table 1. Mosaic analysis of *bendless*

	TTM	DLM
y,w,lz/R(1)w^vc	1.13 (0.09)	1.66 (0.18)
y ben sd f	2.44 (0.41)	1.67 (0.11)
wt head/*ben* thorax	1.05 (0.09)	1.63 (0.14)
ben head/wt thorax	2.31 (0.68)	1.52 (0.17)

Head and thoracic cuticular phenotypes were determined by the markers *yellow* and *forked*. From the mosaic fate map, the brain and head cuticle correlate closely in genotype, thus providing an index to the genotype of the cell body of the GF. Wild-type (wt) tissues are of the genotype *y ben sd f/R(1)w^vc*, while mutant tissues are of the genotype *y ben sd f*. All latency values are in milliseconds. SDs are in parentheses.

fect, abnormal photochoice. Normal flies (CS) strongly prefer UV light over visible light (UV:visible = 25:1). In this behavior, *ben*^{1} flies are abnormal: they prefer visible light over UV (UV: visible = 1:1.3). Interestingly, *ben*^{1} flies are not completely UV blind, such as *sevenless* flies (Ballinger and Benzer, 1988). In *sevenless*, mutants also prefer visible light over UV but in ratios similar to responses seen in the total absence of a UV stimulus (UV:visible or dark:visible = 1:9).

The *ben*^{1} photochoice abnormality suggested a defect in photoreceptor R7, the major UV sensing cell, and prompted us to examine the structure of the eye. Indeed, electron microscopy revealed abnormalities in R7 cells in which the rhabdomere appears deformed and displaced (Fig. 3*F*). Less severe abnormalities were also seen in the rhabdomeres of the other photoreceptor cells. Defects are also present in the lamina (first optic ganglion) where the normally ordered arrangement of the optic cartridges appears completely disrupted (Fig. 3*G*). Despite these defects in the rhabdomeres and the lamina, many R7 and R8 photoreceptor axons project to the medulla (Fig. 3*H*). These axons, however, make shallow disordered projections into the medulla. The origin of these defects can be observed during visual system development at the third instar larval stage. The developing photoreceptor axons of *ben*^{1} flies fasciculate and project from the eye disk through the optic stalk. After exiting the optic stalk, however, the projections appear irregular and disordered (Fig. 3*E*).

There are interesting similarities between the R7 and R8 axonal defects and the GF axonal defect; the mutant phenotype is limited to a bend close to the site of termination. In the case of the GF, a lateral bend that would bring it into proximity with the jump muscle motor neuron is altered. For the R7 and R8 axons, a turn at the surface of the medulla, which would establish the medulla columnar pattern, appears to be aberrant. These findings support an interesting speculation that many neurons require *ben* activity for normal projection of axons in the vicinity of their targets. Thus, *ben* specificity appears to be somewhat different than envisioned by Wyman and Thomas (1983), who implied that use of the gene product might be limited exclusively to the GF-TTMmn connection.

Mosaic analyses of ben^1 *indicate abnormal growth cone physiology*

In *ben*^{1} flies, much of the GF axonal projection is apparently normal: the axon extends normally from the cell body, through the brain, the circumesophageal connective, the cervical connective, the prothoracic neuromere, and into the mesothoracic neuromere (Koto et al., 1981). The total extent of this normal projection is about 500 μm. The *ben*^{1} GF abnormality is limited to the terminal bend representing only about 30 μm of the GF projection. The GF abnormality could be due to a problem in the mesothoracic neuromere. For example, recognition cues in the region of GF-TTMmn connection could be missing or inappropriate. Alternatively, the GF growth cone could misinterpret cues or mount an inappropriate physiological response. That is, we may ask, is the *ben*^{1} phenotype a consequence of the GF genotype or the target region genotype? These two general alternatives should be distinguishable by examining genetic mosaics, particularly head versus thorax mosaics. Mosaics (gynandromorphs) generated from unstable ring X chromosome [*R(1)w^vc*] loss during early embryonic development are useful for our analysis (Hotta and Benzer, 1972; Kankel and Hall, 1976; see Materials and Methods). Tissues originating from cells that retain the ring chromosome during development are wild type (*ben*$^+$), while tissues originating from cells that lose the ring chromosome are mutant (*ben*$^-$).

Mosaic analysis suggests that the GF system phenotype is determined by the genotype of the head, which contains the cell body of the giant axon (Table 1). Thus, most mosaic animals with mutant head and wild-type thorax are phenotypically mutant. Correspondingly, mosaic animals with a wild-type head and a mutant thorax are phenotypically wild type. Our interpretation is that a mutant GF cannot make a connection with a normal TTMmn while a normal GF can enter the *ben*^{1} target region and make a connection with a *ben*^{1} TTMmn. Since the site of misconnection (mesothoracic ganglion neuropil) is physically remote from the apparent genetic focus of the defect (somewhere in the head, probably the GF cell body), *ben*^{1} probably corresponds to a presynaptic GF defect involving a growth cone dysfunction.

←

Figure 3. Visual system abnormalities in *ben*^{1} mutant. The *Drosophila* retina contains about 800 ommatidia. The eight photoreceptor neurons of each ommatidium project in a stereotyped pattern to the optic ganglia. Axons from photoreceptor cells R1 to R6 synapse in the optic cartridges of the lamina, the first optic ganglion. Fibers from R7 and R8 pass through the lamina without making synaptic contacts, continuing through the first optic chiasm to make synapses in the second optic ganglion, the medulla. The medulla has a characteristic columnar organization with inputs coming from R7 and R8 axons and lamina interneurons, and output via the medullary neuron. Wild-type CS (*A–D*) and *ben*^{1}/*Df(1)HA92* (*E–H*). *A* and *E*, Third instar larvae eye imaginal disk and brain. Photoreceptor axons are stained with mAb 22C10 and FITC-conjugated secondary antibody. Bundles of axons from the developing photoreceptor clusters in the eye disk project through the optic stalk and onto the larval brain where they connect to the developing optic lobe. In a *ben*^{1} fly, these projections are irregular. *B* and *F*, Adult eye. Tangential sections seen at the electron microscopic level show the arrangement of rhabdomeres in wild-type, which is precisely reiterated from facet to facet; R7 projects into the center of the group. A *ben*^{1} mutant shows frequent abnormalities in the spacing and size of the rhabdomeres, particularly in R7 (*arrows*). *C* and *G*, Adult lamina (the first optic ganglion) in electron microscopic section. In wild type, this is a regular arrangement of optic cartridges, each with large postsynaptic lamina (*L*) neurons at the center surrounded by six photoreceptor axons (*R*). This arrangement is highly distorted in the *ben*^{1} mutant. *D* and *H*, R7 and R8 photoreceptor projection patterns in the medulla (second optic ganglion). The fibers are seen in horizontal section and visualized by HRP filling. The columnar organization of the wild-type medulla is evident from the staining pattern. In a *ben*^{1} fly, fibers reach the medulla but make aberrant shallow projections into the neuropil (*arrow*).

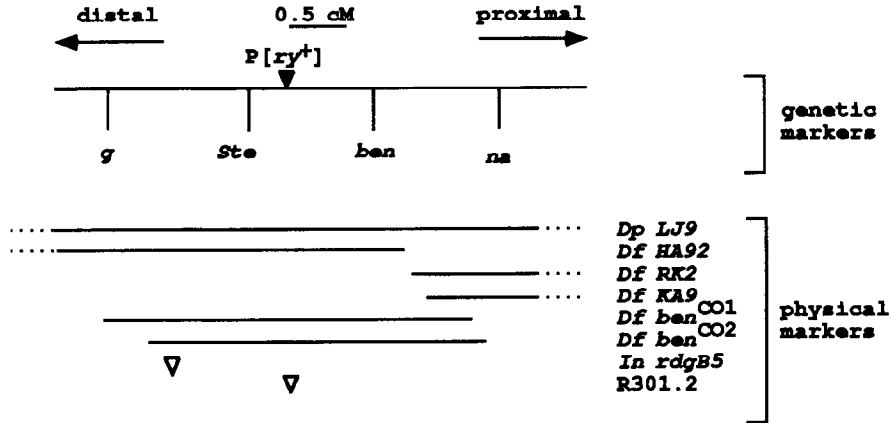

Figure 4. Genetic location of *ben* in the 12D region of the X chromosome. The *ben* gene maps by recombination between *g* (44.4) and *na* (46.5) at map position 45.8 as determined from the *g-ben* interval (1.4 cM). Physically, *ben* is flanked on the left by the transposon insertion of the R301.2 chromosome (location 12D, labeled "P[ry^+]"), and on the right by the proximal breakpoint of the *Df(1)HA92* deletion (12A6-7 to 12D3). The *ben* gene is covered by the duplication of *Dp(1)LJ9* (12A6 to 13A2-5). It is uncovered by the deletions *Df(1)HA92* (12A6-7 to 12D3), *Df(1)ben*^{CO1} (12B7 to 12E3), and *Df(1)ben*^{CO2} (12C5-6 to 12E6). It is not uncovered by the deletions *Df(1)RK2* (12D2-E1 to 13A2-5) and *Df(1)KA9* (12E2-3 to 12F5-13A1). Other recombination distances in the *ben* region include the *g–na* interval (2.5 cM), the *ben–na* interval (1.2 cM), and the P[ry^+]–*ben* interval (0.7 cM).

Genetic and molecular cloning of ben

The *ben*^{1} mutation mapped to the 12D region of the X chromosome (Fig. 4). The relationships among *ben*^{1} and several markers in and around 12D were determined. Most notably for subsequent discussions, *ben*^{1} is uncovered by the *Df(1)HA92* deletion and is 0.7 cM (centimorgan) proximal to the R301.2 P-element transposon insertion.

The *ben* gene was cloned in a chromosomal walk through the 12D region of the X chromosome that covered 290 kb of overlapping phage and cosmid clones. The walk, initiated from the transposon insertion site of R301.2, extended bidirectionally until we determined a proximal–distal orientation by *in situ* hybridization to salivary gland polytene chromosomes and by localization of the *rdgB* breakpoint mutation *In(1)rdgB5* (Vihtelic et al., 1991). The walk continued proximally until restriction fragment length polymorphism (RFLP) analysis, as described below, indicated that *ben* had been cloned. Figure 5 shows the relevant 200 kb of the proximal walk.

To localize the *ben* transcription unit, male +;ry^{42} recombinants derived from *ben*^{1} *sd f/wy* R301.2;ry^{42} female flies were scored for presence of the *ben*^{1} *sd f* chromosome with RFLPs situated at various points on the chromosomal walk. Extrapolation of the recombination frequency derived from the RFLP analysis localized *ben* to approximately 172 kb from the R301.2 insertion site (Fig. 6*A*; van der Bliek and Meyerowitz, 1991). A probe of polyA$^+$ RNA from various stages of development with DNA fragments from +150 to +200 kb revealed several transcripts in the area (Fig. 6*B*). Two of the transcripts were good candidates for *ben* based on location: a 6 kb transcript (D2) at +168 kb and several similarly sized 1.9 kb transcripts (D3) at +175 kb. The 6 kb transcript is restricted in expression to the first and second larval stages of development while the 1.9 kb transcripts are expressed throughout all developmental periods,

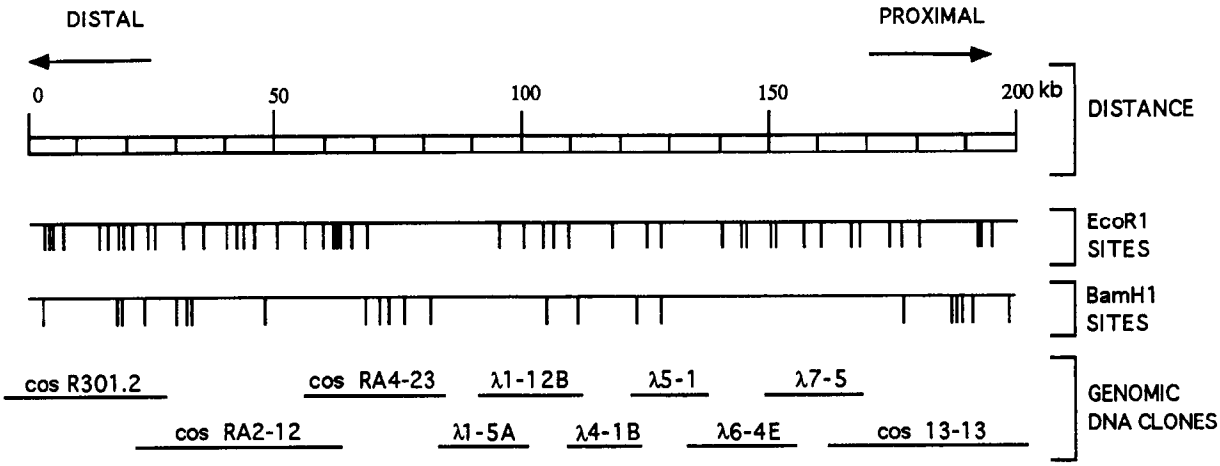

Figure 5. Restriction maps of the *ben* region and genomic DNA clones obtained from chromosomal walking. Starting from the transposon insertion site of R301.2, overlapping DNA clones were isolated from genomic DNA libraries constructed in bacteriophage lambda and cosmid vectors. Unique DNA sequences of identified clones were used to isolate additional genomic DNA clones, thereby extending the walk bidirectionally. The total walk encompassed about 290 kb: from −50 kb to +240 kb. For simplicity, only representative clones from the proximal 200 kb are depicted. Restriction maps are the cleavage sites for EcoRI and BamHI. Distances from R301.2 are shown in kilobases.

with heightened expression at the pupal stages (Fig. 6*C*). Because of mutant effects on the GF and the visual system, *ben* must be active during the period of retinal innervation of the optic lobes and development of the GF at the late third larval and early pupal stages of development (Wyman et al., 1984; Steller et al., 1987; Selleck and Steller, 1991). This indicated that the 1.9 kb transcripts were good candidates to be *ben*.

The *ben* gene was positively identified by P-element–mediated germ line transformation. A 6 kb XhoI fragment and an 18 kb genomic phage clone that encompass the 1.9 kb transcripts were separately introduced into flies (Fig. 6*B*), and established transformant lines crossed to *w m ben*^{1} flies. The resulting *w m ben*^{1};P[w^+] progeny carrying either genomic DNA fragments recovered wild-type levels of viability and locomotor activity. All transgenic flies jumped normally (45–55% jumpers) and showed a normal photochoice response (UV:visible = 25:1 and dark:visible 1:11.5). In contrast, control *w m ben*^{1} flies failed to jump (0% jumpers) and displayed abnormal photochoice (UV:visible or dark:visible = 5:1). Electrophysiological examination of the TTM responses showed complete rescue of the *ben* phenotype: the latency of the TTM was restored from an average value of 3.37 msec for *ben*^{1} flies to wild-type values of 1.07 msec for the transgenes (Fig. 7, Table 2). Even under higher stimulus rates at which the TTM response completely fails in *ben*^{1} flies, the transgenes show normal responses. Correspondingly, the morphology of the GF in these flies is normal and displays the characteristic lateral projection typical of a wild-type GF (Fig. 7*B,C*). Dye coupling between the GF and TTMmn in the transgenes indicates the formation of a functional electrical synapse between the two neural elements. The recovery of all normal phenotypes provides firm evidence that the 1.9 kb transcripts encode the *ben* gene product and that 6 kb of genomic DNA contains the complete transcription unit.

ben *is homologous to ubiquitin-conjugating enzyme*

Complementary DNAs derived from the 1.9 kb *ben* transcripts were isolated using a 3.5 kb EcoRI genomic fragment. A screen of embryonic and pupal cDNA libraries yielded clones ranging from 0.5 to 1.9 kb. A 1.8 kb clone from an embryonic library and a 1.9 kb clone from a pupal library, both hybridizing to the 3.5 kb EcoRI fragment in genomic Southerns (data not shown), were sequenced. The two cDNAs differ in their noncoding 5′ sequences, but are nearly identical throughout with one long open reading frame of 453 base pairs (Fig. 8). The deduced amino acid sequence reveals strong homology to ubiquitin-conjugating enzymes (UBCs), a class of proteins that transfer ubiquitin moieties to a variety of protein targets (Hochstrasser, 1992; Jentsch, 1992). Best homology is observed for the yeast enzyme (UBC5) and a *Drosophila* homolog (UBC4-DROME) with identical matches of 48% (Fig. 9). Other UBCs homologous to *ben* include yeast UBC4, *Arabidopsis thaliana* and wheat UBC1, and human UBC2 (Seufert and Jentsch, 1990; Koken et al., 1991a; Sullivan and Viestra, 1991).

All UBC genes code for a small protein of 16–21 kDa containing a characteristic globular catalytic "core" domain (Cook et al., 1992). The unique features of this "core" domain are present in the putative *ben* polypeptide. For example, a conserved cysteine residue found in all UBCs forming the thiolester bond with ubiquitin is present at residue 87 (Sullivan and Vierstra, 1991). The sequence surrounding this cysteine is highly conserved between UBCs and *ben*. In addition, a proline residue, whose substitution by serine converts yeast RAD6 and

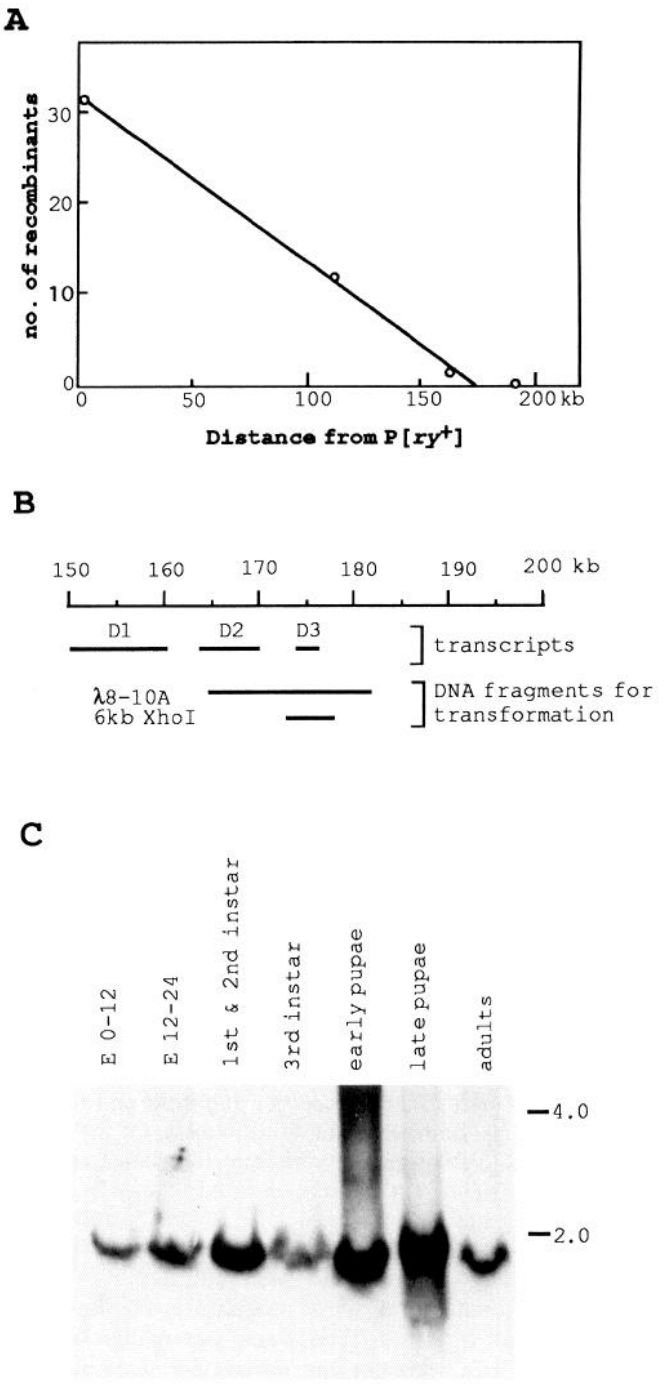

Figure 6. Localization of *ben* and identification of transcripts. *A*, The number of recombinants carrying the *ben sd f* chromosome, as determined by RFLP analysis, is plotted as a function of distance from the distal marker R301.2. The x-intercept, corresponding to the location of *ben*, is at +172 kb. Note the absence of any recombinants farther than +195 kb. *B*, Transcripts identified from the +150 to +200 kb region. The *D1* transcripts with size ranges of 3–8 kb are expressed throughout development. *D2* is a 6 kb transcript restricted to the first and second larval instar stages. *D3*, consisting of several similarly sized 1.9 kb transcripts, is expressed throughout all stages of development. Also shown are genomic DNA fragments used for P-element transformation experiments. *C*, Expression profile of the D3 transcripts. Each lane contains 20 μg of polyA$^+$ RNA isolated from the indicated developmental stages. *E 0–12* and *E 12–24* are embryonic stages given in hours after egg laying. The probe is a 3.5 kb EcoRI genomic fragment that covers most of the D3 transcription unit. RNA length size standards are in kilobases.

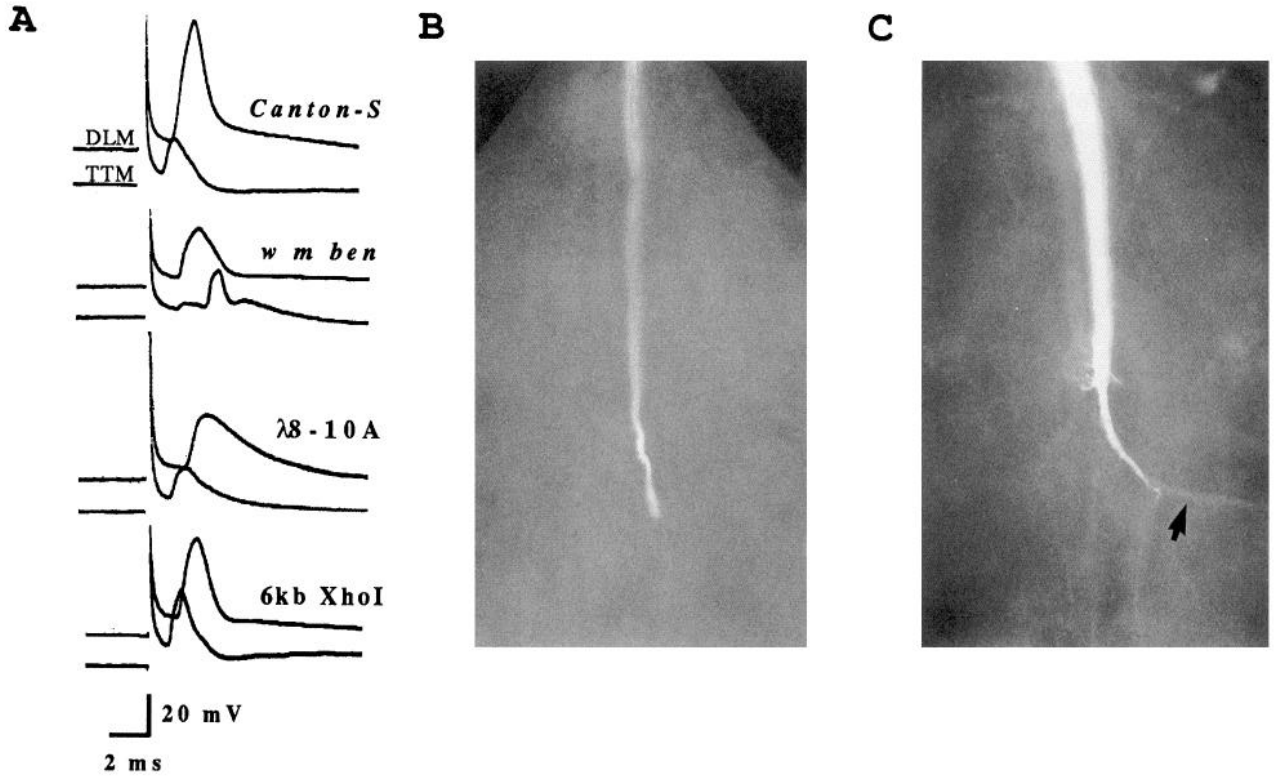

Figure 7. Rescue of the *ben*^{1} phenotype by genomic DNA fragments. *A*, Single DLM (*upper traces*) and TTM (*lower traces*) recordings from wild-type (CS), *w m ben*^{1} and *w m ben*^{1};P(w^+) flies. The transgenes carry the 6 kb (XhoI) or 18 kb (λ8-10A) genomic fragment encompassing the 1.9 kb transcripts. *B* and *C*, Morphology of the GF in *w m ben*^{1} and *w m ben*^{1};P(w^+T25). Lucifer yellow dye injection reveals the abnormal GF axon in the mesothoracic neuromere of a *w m ben*^{1} fly: the GF extends only a short distance beyond its connection with the PSI. In a transgenic fly carrying the 6 kb XhoI fragment, the GF connects with the PSI and then continues to extend laterally as in wild-type. Note that dye coupling between the GF and the TTMmn is clearly evident in *C* but not in *B* (*arrow*).

CDC34 to temperature sensitive mutants, is present at residue 63 (Ellison et al., 1991). This proline is conserved in all UBCs and constitutes part of a turn between the third and fourth β sheets of the core domain (Cook et al., 1992). Of the known types of UBCs, *ben* appears to represent the class I enzymes because it lacks significant carboxy-terminal extensions present in class II enzymes such as yeast UBC1, UBC3, and UBC6 (Jentsch, 1992). These carboxy-terminal extensions, with rather diverse sequences, are believed to specify interactions with target proteins and allow transfer of ubiquitin in the absence of accessory factors. In contrast, class I enzymes mainly consist of the conserved UBC domain and are inefficient at ubiquitin transfers when tested *in vitro*. Class I enzymes may require auxiliary proteins, ubiquitin-ligases (UBRs), to interact with various acceptor proteins (Sharon et al., 1991).

Discussion

We have molecularly cloned the *Drosophila ben* gene and shown that its product is related to a class of UBCs. This leads to a rather surprising conclusion that ubiquitination may play an important role in neural development and growth cone physiology. Here we discuss arguments leading to this conclusion and speculate about the developmental processes in the nervous system that ubiquitination might be affecting.

ben *affects many neural connections*

The original *ben*^{1} mutation was isolated as a neuronal connectivity mutation thought to be specific for a single synapse within the *Drosophila* nervous system, the GF and the its connection with the TTMmn, since no other defects were observed (Wyman

Table 2. P-element rescue of *bendless*

	1 stimulus/sec		5 stimuli/sec	
	TTM	DLM	TTM	DLM
Canton-S	0.96 (0.09)	1.61 (0.10)	1.08 (0.05)	1.79 (0.07)
w m ben	3.37 (1.03)	1.80 (0.14)	NR	1.98 (0.15)
w m ben;P[w^+T25]	1.07 (0.10)	1.57 (0.11)	1.22 (0.05)	1.90 (0.12)
w m ben;P[w^+T65]	1.18 (0.10)	1.80 (0.10)	1.26 (0.10)	1.92 (0.13)

Latency values are in milliseconds and ± SDs are in parentheses. All flies tested were males. The P[w^+T25] carries the 6 kb XhoI fragment while P[w^+T65] carries the 18 kb genomic fragment. NR, no response.

```
CCCCCCCCCC CCATAATTTT TGTGGTGGAG CTGCCTGCAA AATCGAATTT TATCAGTTTG CCAACGAAGT TATCGGCCAT   80
AACTGCAAAT AAAGTTTAGC AATAACTTGG CGCTGTTACG ATCTCAACGA GAAGGTCCAG ACTCAACCCG CGTTTCCAGT  160
TCACCGCGTA AAAGGAACCA GCTAAACG  ATG TCC AGC CTG CCA CGT CGC ATC ATC AAG GAG ACT CAA CGT  230
                                M   S   S   L   P   R   R   I   I   K   E   T   Q   R   14
TTG ATG CAG GAG CCA GTG CCT GGG ATC AAT GCC ATT CCC GAT GAG AAC AAT GCC CGT TAC TTC CAT  296
 L   M   Q   E   P   V   P   G   I   N   A   I   P   D   E   N   N   A   R   Y   F   H  36
GTG ATC GTG ACC GGA CCG AAC GAT TCG CCC TTC GAG GGC GGC GTG TTC AAG CTG GAG CTG TTC CTA  362
 V   I   V   T   G   P   N   D   S   P   F   E   G   G   V   F   K   L   E   L   F   L  58
CCG GAG GAC TAT CCA ATG TCA GCG CCC AAA GTG CGC TTC ATC ACG AAG ATC TAC CAT CCG AAC ATC  428
 P   E   D   Y   P   M   S   A   P   K   V   R   F   I   T   K   I   Y   H   P   N   I  80
GAT CGT TTG GGC CGC ATT TGC CTC GAC GTG CTG AAG GAC AAG TGG AGT CCA GCC CTG CAG ATC CGG  494
 D   R   L   G   R   I   C   L   D   V   L   K   D   K   W   S   P   A   L   Q   I   R  102
ACC ATA TTG CTA TCC ATT CAG GCA CTG CTC AGT GCA CCC AAT CCC GAC GAT CCG CTG GCC AAC GAT  560
 T   I   L   L   S   I   Q   A   L   L   S   A   P   N   P   D   D   P   L   A   N   D  124
GTG GCT GAG TTG TGG AAG GTC AAC GAG GCG GAG GCC ATT CGC AAT GCC CGC GAG TGG ACC CAG AAA  626
 V   A   E   L   W   K   V   N   E   A   E   A   I   R   N   A   R   E   W   T   Q   K  146
TAT GCC GTC GAA GAC    TGAACGCCC GAGGTCAGGA GGAAAGTCAG AAAGCGGATC CGTCAGTTGT ATCGGCGTTT  700
 Y   A   V   E   D                                                                     151
TTCCAGAAAG TGGGTGCGTG ACATGAACGG GCGGGTGGGT AAATTGAATA CTTTAAAAGC AACCAGAAAA ACCTAAAACA  780
TACGAAAGAA AACATAAAAT AAGAAAAAAG TAAGCAAGCA AACATAAAAA AAAACGATTT AAGAACACAT TTTTTTTTCG  860
AACCTTCTGG GGCGGGATAT ACATATAAAA TATTAATATA TATATTTTTT TCAACCAATC GATCGGGGCG ATCGGCGAAA  940
TGGAGGAGAG ATAGCGAAAG CATTCTTTAT GTAAGACGTA TACATGTATC CGAAACAAAC TAAAAACGAA AAAAAAAAAA 1120
AAAAAAACAG TAATTGGTTT TAGTCGTTTC TATTGATTTG TTCGAGGGTT CTGGTGTCTA TATACATATA GCCGTATATA 1200
ATTCTATGTG TAACTGAAAT AACCAACCCA TAACCATTAA CACATGTAGC ATCAGATATG ATAAATCAAT TGGAAAGGCA 1280
AACAAGAAGG GATTTTGATT TCCTTTAACT CGTCATTTGA AAACTCGGCT TAAATGTCAA TTCAAAATAG AGAATTTTGA 1360
TTGTATCATT TTCAGTGTTT CAGAAAATTT AAGATGTGAT CGTCCAACTT GTAGACTTTA CTTTTCTTAA CTAAGAGTTC 1440
ACCATTTCGA TTGATACTTG AGCTTTGCCT GGGTTGTGTC AGAGTCCCTT TGATAAACGA TAAATAGTTT TTACTCGAAA 1520
ACAATTTTTT TTAACCAAAC AATGAAGCCT TTAAGCTATT AGTAATTTTT GAAAAAAAAA ATAAAAAATA TATATATAAA 1600
AAATATACAA AAATATGATA CATGATCAAA ATACAATGAA TGCATACACT ATATATTTAT ACAAAAAAAA TACAAAAAGA 1680
AAAACAAAAG TAGTGGCTTG ATTGCGTGAA AATTTCAAGT GCAGTTCTCA ACAAAAATTG TGTACAGTAA TTAAATGTTT 1760
GTCACCGAAA TCACTAAAGG ATAATCCAAA AAACAATAGC AACCGAAAAG CAACCATAAA TAAAAGAGTA AGCGAAAATA 1840
AAAATTCAGT TTTCTTTAAT TTTAATTAAT TTTTTTTCTA AGAAAAATAA ATAAAAACGA AAAATTCAAA TAAAAATTAT 1920
AAAAAATAAA AAAAAAAAAA AAAAAAAAAA                                                      1950
```

Figure 8. Nucleotide and deduced amino acid sequence of *ben*. Presented is the complete nucleotide sequence of the 1.9 kb pupal cDNA clone and its corresponding translation product. A cDNA isolated from an embryonic library (not shown) is divergent up to nucleotide residue 123 of the pupal clone, but thereafter identical until residue 825. The 3′ noncoding region of the embryonic cDNA differs only by shorter polydA tracts initiating at nucleotide residues 826, 1008, and 1471 of the pupal cDNA. Priming from internal polyA tracts during cDNA construction appears to account for a number of shorter clones whose 3′ ends are located internally of the larger cDNAs.

and Thomas, 1983). However, present observations indicate that *ben* defects are substantially more widespread. We have shown that *ben*[1] causes abnormal projections of the R7 and R8 retinal axons in the medulla optic ganglion. By examination of eye imaginal disk–brain preparations in third instar larvae, we found that this abnormality occurs early and is not due to a late retraction of previous correct synapses. There are also defects in the lamina and the photoreceptor cells, which have abnormally shaped rhabdomeres. R7 in particular is badly deformed, possibly accounting for the abnormal color choice of *ben* flies. Previous studies show that proper development of the optic ganglia and survival of photoreceptor neurons are dependent on retrograde and anterograde interactions between the two structures (Meyerowitz and Kankel, 1978; Selleck and Steller, 1991; Campos et al., 1992). It is unclear whether the *ben*-induced defects in the lamina and the rhabdomeres are due to

```
MSSLP-RRIIKETQRLMQEPVPGINAIPDENNARYFHVIVTGPNDSPFEGGVFKFELFLPEDYPNSAPKVRFITKIY  BEN
MSS--SKRIAKELSDLGRDPPASCSAGPVGDDLYHWQASIMGPSDSPYAGGVFFFSIHFPTDYPFKPPKVNFTTKIY  UBC5-YEAST
M---ALKRINKELQDLGRDPPAQCSAGPVGDDLFHWQATIMGPPDSPYQGGVFFFTIHFPTDYPFKPPKVAFTTRIY  UBC4-DROME
MSS--SKRIAKELSDLERDPPTSCSAGPVGDDLYHWQASIMGPADSPYAGGVFFFSIHFPTDYPFKPPKISFTTKIY  UBC4-YEAST
MSTPARKRLMRDFKRLQQDPPAGISGAPHDNNITLWNAVIFGPDDTPWDGGTFKFTLQFTEDYPNKPPTVRFVSRMF  UBC1-WHEAT
MSTPARKRLMRDFKRLQQDPPAGISGAPQDNNIMLWNAVIFGPDDTPWDGGTFKFSLQFSEDYPNKPPTVRFVSRMF  UBC1-ARATH
MSTPARRRLMRDFKRLQEDPPTGVSGAPTDNNIMIWNAVIFGPHDTPFEDGTFKFTIEFTEEYPNKPPTVRFVSKVF  UBC2-DHR6
MSTPARRRLMRDFKRLQEDPPVGVSGAPSENNIMQWNAVIFGPEGTPFEDGTFKFVIEFSEEYPNKPPTVRFLSKMF  UBC2-HUMAN

                *
HPNIDRLGRICLDVLKDKWSPALQIRTILLSIQALLSAPNPDDPLANDVAELWKVNEAEAIRNAREWTQKYAVED  BEN
HPNINSSGNICLDILKDQWSPALTLSKVLLSICSLLTDANPDDPLVPEIAQIYKTDKAKYEATAKEWTKKYAV   UBC5-YEAST
HPNINSNGSICLDILRSQWSPALTISKVLLSICSLLCDPNPDDPLVPEIARIYKTDREKYNELAREWTRKYAM   UBC4-DROME
HPNINANGNICLDILKDQWSPALTLSKVLLSICSLLTDANPDDPLVPEIAHIYKTDRPKYEATAREWTKKYAV   UBC4-YEAST
HPNIYADGSICLDILQNQWSPIYDVAAILTSIQSLLCDPNPNSPANSEAARMYSENKREYNRKVREVVEQSWTAD  UBC1-WHEAT
HPNIYADGSICLDILQNQWSPIYDVAAILTSIQSLLCDPNPNSPANSEAARMYSESKREYNRRVRDVVEQSWTAD  UBC1-ARATH
HPNVYADGGICLDILQNRWSPRYDVSAILTSIQSLLSDPNPNSPANSTAAQLYKENRREYEKRVKACVEQS-FID  UBC2-DHR6
HPNVYADGSICLDILQNRWSPTYDVSSILTSIQSLLDEPNPNSPANSQAAQLYQENKREYEKRVSAIVEQS-WNDS  UBC2-HUMAN
```

Figure 9. Homology of *ben* to UBCs. Residues identical among the proteins are shown in reverse type. The conserved cysteine residue that acts as the ubiquitin acceptor is indicated by an *asterisk*. All alignments begin at initiating methionines. Alignments were generated by the GENALIGN program (Intelligenetics, Inc.). The amino acid sequences of UBC homologs are from the following: *Drosophila melanogaster* UBC4 (Treier et al., 1992), yeast UBC4 and UBC5 (Seufert and Jentsch, 1990), *Drosophila melanogaster* Dhr6 (Koken et al., 1991a), *Arabidopsis thaliana* and wheat UBC1 (Sullivan and Viestra, 1991), and human UBC2 (Koken et al., 1991b).

degeneration of these structures in the absence of *ben*$^+$ activity or due to the absence of functional photoreceptor cell–optic ganglion interactions.

In addition to the effects on the visual system, we suspect other aspects of development may also be affected. The relative abundance of the *ben* transcript, its expression at all stages of development, the variety of behavioral deficits in *ben*^{1} flies (inability to groom, jump, phototax, and eclose properly), and abnormalities in the thoracic musculature (Edgecomb et al., 1993) all suggest a broader activity of *ben*$^+$ in nervous system function, and possibly, general development.

We are uncertain about which nervous system deficits are responsible for the jump abnormality since the *ben*^{1} mutation is pleiotropic. The main escape jump in *Drosophila* is driven by a visual stimulus via the GF system. The behavioral abnormality could therefore be due to the GF-TTMmn alteration as originally described. However, the visual system alterations described here might also contribute substantially to this behavioral deficit. This possibility is suggested by the ability of the GF in *ben*^{1} flies to drive the TTM, albeit via a long-latency, highly labile pathway. It is curious that the TTM response occurs despite the absence of an anatomically identifiable contact between the GF and the TTMmn. The *ben*^{1} GF-TTM response superficially resembles a normal GF-DVM I or GF-DVM II response. However, the possibility that the mutant GF uses one of these pathways to drive the TTM seems unlikely since those responses appear to be mediated via different neuronal pathways (Fig. 2*E,F*; Tanouye and Wyman, 1980). Another possibility is the existence in wild-type flies of a normal long-latency parallel pathway between the GF and TTMmn that is masked by feed-forward inhibition. However, there is presently no evidence for such a pathway and it is unclear what function it would serve. Most likely, the *ben*^{1} GF-TTM response is due to an abnormal pathway arising *de novo* in the mutant.

Specificity of ben^1 *phenotypes*

Despite the indication that many neurons are affected by *ben*, there is also a degree of specificity associated with the lesion. As it affects the GF, the defect is apparently limited to its terminal projection. The GF axon projects far from its cell body, through a complex pathway, to its target region. It fails to make one final turn that would bring it to its normal TTMmn termination site. Interestingly, all other GF outputs are intact; outputs to the DLM, DVM III, and probably also DVM I and DVM II, appear normal. Thus, the deficit, within the GF itself, is very specific, affecting only a single output. Photoreceptor axons also appear to initially project properly through the optic stalk, but later behave abnormally. In the case of photoreceptors R7/R8, many axons project to the vicinity of their targets in the medulla. However, they fail to turn and project deep into the medulla optic ganglion. Thus, in the GF and R7/R8 axons, *ben* may act to regulate the direction of axon growth near the postsynaptic target. Whether similar or different morphological defects are present in axonal projections of other neurons await their detailed analyses in *ben*^{1} flies.

ben *and the ubiquitination pathway*

The formation of ubiquitin-protein conjugates is a multistep process involving an activating enzyme (UBA), a family of UBCs, and UBRs. If *ben* acts in the development of many neurons, how does this relate to its putative biochemical function as a UBC?

UBCs homologous to *ben* are a diverse family that transfer ubiquitin from UBA to specific cellular proteins (Jentsch, 1992). Much biochemical and genetic evidence shows that the ubiquitination pathway affects a range of cellular processes including the cell cycle, DNA repair, peroxisome biogenesis, and protein secretion by targeting proteins for degradation (Jentsch et al., 1987; Laszlo et al., 1990; Herschko, 1991; Hochstrasser, 1992; Kolman et al., 1992; Wiebel and Kunau, 1992). The targets of UBCs, reflecting their role in cellular control, include a variety of regulatory proteins: Matα2 repressor, p53, cyclin (Glotzer et al., 1991; Rechsteiner, 1991), T-cell antigen receptor (TCR), IgE receptor, and platelet-derived growth factor receptor (Yarden et al., 1986; Cenciarelli et al., 1992; Paolini and Kinet, 1993). For receptors, modification is dynamic, with ubiquitination occurring within seconds after ligand binding and deubiquitination taking place rapidly upon ligand dissociation. Although modifications of membrane proteins are also believed to be mechanisms for their selective degradation (Mori et al., 1992), use of transient ubiquitinations in modulating signal transduction cascades has also been suggested (Paolini and Kinet, 1993).

ben is the third putative UBC gene to be identified in *Drosophila*. UbcD1 (UBC4-DROME) and Dhr6 were isolated by their sequence homology to yeast UBC4 and RAD6 genes, respectively (Koken et al., 1991b; Treier et al., 1992). Both *Drosophila* UBCs can partially or fully complement mutations in their respective yeast homologs. What exact cellular functions Dhr6 and UbcD1 regulate *in vivo* are unknown since no mutations have been identified. However, the presence of these other *Drosophila* UBCs appears insufficient to complement the neural development and connectivity function of *ben*. Thus, the activities of *ben* and other UBCs may differ in their target specificities or tissue expression patterns.

Role of ben *in neural development and growth cone physiology*

If *ben* is an UBC, how does it affect neural development and axon guidance? Although some of the phenotypes may be due to a general defect, such as a deficiency in bulk protein degradation, this explanation does not fit neatly with the all the observed phenotypes. A difficult albeit the most interesting feature to explain is why axon outgrowth in the mutants appears initially normal for a rather long distance, and then fails near the target. In the GF, mosaic analysis argues that the focus of *ben*^{1} defect is the GF and not the target; this presynaptic defect very likely affects the developing growth cone.

Some explanations for *ben* activity in the developing growth cone appear unlikely, such as actions involving cytoskeletal elements or general neurite outgrowth (Ball et al., 1987; Murti et al., 1988; Hondermarck et al., 1992). If these were at play, one would not expect the GF to be capable of making normal outputs in all cases except for the connection to the TTMmn, or the photoreceptor axons R7/R8 to be capable of projecting through the optic stalk to the medulla optic ganglion.

To account for the specificity of the *ben* axonal defects, the most plausible targets are molecules such as receptors involved in cell–cell interaction. Ubiquitination of receptors or their associated signal transduction elements presents a salient mechanism by which a neuronal growth cone could be guided along the pathway toward its postsynaptic partner. Specific defects occur when the growth cone is unable to regulate specific interactions with guidance cues present at various points in the axon

pathway. An alteration in cell–cell interaction might also explain many of the other phenotypes found in *ben*^{1} mutants.

Several models can be proposed to explain how ubiquitination regulates axon guidance. One model arises from the rapid ubiquitination/deubiquitination cycles observed for TCR and IgE receptors (Cenciarelli et al., 1992; Paolini and Kinet, 1993). Although concrete evidence is lacking, such transient modifications are implicated in regulating signal transduction pathways. If operative, ubiquitin-mediated signaling mechanisms could activate or stabilize adhesive interactions that allow the growth cone to extend toward its target. Ubiquitination of receptors is triggered by binding of the ligand with the receptor. An ensuing intracellular signal (e.g., an activated receptor kinase), initiated or influenced by ubiquitination, may modify adhesion molecules such as integrins, increasing their affinity for specific ligands (Hynes, 1992). The changes in affinity would redirect the migration of the growth cone. Such "adhesion cascade" mechanisms have been proposed to explain the diversity of cell–cell and cell–matrix interactions mediating the adhesion of platelets, receptor-dependent triggering of lymphocytes, and neurite outgrowth (Doherty et al., 1991; Phillips et al., 1991; O'Rourke and Mescher, 1992; Schweighoffer and Shaw, 1992). In *ben*^{1} flies, a defect in modulating the signal transduction cascade by ubiquitination could result in a growth cone being unable to continue along the correct pathway. Curiously, double mutants of UBR1 and phosphotyrosine phosphatase (PTP2) in yeast display a lethal phenotype although independent mutations in either UBR1 or PTP2 do not (Guan et al., 1992; Ota and Varshavsky, 1992). This is suggestive of some interplay between the ubiquitination pathway and the phosphorylation-mediated cell-signaling cascade. Provocative as they may be, models involving ubiquitin-regulated cell signaling mechanisms await further studies.

A second model, which appears more plausible based on the known functions of ubiquitination, is the requirement of *ben*$^+$ for degradation of proteins involved in inhibitory or repulsive cell–cell interactions. Recent studies have identified repellent or antiadhesive mechanisms for axon guidance in such systems as spinal nerve segmentation and retinotectal projection (Kapfhammer and Raper, 1987; Patterson, 1988; Walter et al., 1990). An avoidance reaction of neurites can be induced by glycoproteins from the posterior half of a somite and posterior tectal membranes (Cox et al., 1990; Davies et al., 1990), thereby guiding the direction of axon growth. The oligodendrocyte-derived J1-160/180 family of extracellular matrix (ECM) glycoproteins also shows repellent or antiadhesive qualities to neurites of cerebellar explant cultures (Faissner and Kruse, 1990; Morganti et al., 1990). Interestingly, disruption by antibodies of the interaction between the J1-160/180 ECM protein and its putative glyco-phosphatidyl–anchored receptor, F3/11, eliminates the repulsive reaction of the neurites (Pesheva et al., 1993). Similarly, we might postulate that in *ben*$^+$-expressing neurons, turnover or downregulation of a specific receptor or related signal transduction element through ubiquitin-mediated degradation is a crucial point of regulation that allows the axon to grow toward the target. For instance, as the GF growth cone maneuvers from the brain to the thoracic ganglia, an antiadhesive receptor–ligand interaction may prevent it from taking lateral pathways. As the growth cone reaches the point in the thoracic ganglion where it must make a lateral turn, the *ben*$^+$ product downregulates or perturbs receptor function, allowing the axon to make a lateral turn. In *ben*^{1} mutants, the inhibitory interaction cannot be specifically downregulated, and thus the mutant GF cannot make a lateral turn. A dynamic cellular structure must continually turn over cellular elements to adjust to the changing environmental cues. Failure to do so would lead to misdirection of the growth cone.

The finding that *ben* encodes a putative UBC suggests new directions for dissecting growth cone function and neural development. Molecular genetic approaches can be used to characterize other UBCs and UBRs participating in specific neural functions. More importantly, one can begin to identify the targets of *ben* ubiquitination, some of which may be molecules (i.e., receptors) responsible for pathway guidance. Target molecules of *ben* may be identified genetically as suppressors or possibly as enhancers of *ben* alleles. From this type of analysis, it should be possible to determine whether *ben* acts on a single molecule or on a collection of molecules that act together to provide redundancy in pathway detection. Taken together, these types of investigations suggest new avenues to examine one of the fundamental problems in neurobiology: identifying the molecules that direct neuronal connectivity.

Note added in proof

During the review of this manuscript, an article by Muralidhar and Thomas (1993) was published that also describes the cloning of the *ben* gene. They cite our earlier unpublished findings that *ben*^{1} has neuronal defects additional to the GF defect and confirm many others of our observations. In addition, their experiments with *ben-bithorax* mutants provide support for the models we have presented.

References

Ball E, Karlik CC, Beall CJ, Saville DL, Sparrow JC, Bullard B, Fyrberg EA (1987) Arthrin, a myofibrillar protein of insect flight muscle, is an actin–ubiquitin conjugate. Cell 51:221–228.

Ballinger DG, Benzer S (1988) *Photophobe* (*Ppb*), a *Drosophila* mutant with a reversed sign of phototaxis; the mutation shows an allele-specific interaction with *sevenless*. Proc Natl Acad Sci USA 85:3960–3964.

Benzer S (1991) Helmerich lecture: the fly and eye. In: Development of the visual system, Vol 3 (Lam DM-K, Shatz C, eds), pp 9–34. Cambridge, MA: MIT Press.

Bier E, Vaessin H, Shepherd S, Lee K, McCall K, Barbel S, Ackerman L, Carretto R, Uemura T, Grell E, Jan LY, Jan YN (1989) Searching for pattern and mutation in the *Drosophila* genome with a P-lacZ vector. Genes Dev 3:1273–1287.

Bovolenta P, Dodd J (1990) Guidance of commissural cones at the floor plate in embryonic rat spinal cord. Development 109:435–447.

Bovolenta P, Dodd J (1991) Perturbation of neuronal differentiation and axon guidance in the spinal cord of mouse embryos lacking a floor plate: analysis of Danforth's short tail mutation. Development 113:625–639.

Campos AR, Fischbach K-F, Steller H (1992) Survival of photoreceptor neurons in the compound eye of *Drosophila* depends on connections with the optic ganglia. Development 114:355–366.

Caudy M, Bentley D (1986) Pioneer growth cone steering along a series of neuronal and non-neuronal cues of different affinities. J Neurosci 6:1781–1795.

Cenciarelli C, Hou D, Hsu K-C, Rellahan BL, Wiest DL, Smith HT, Fried VA, Weissman AM (1992) Activation-induced ubiquitination of the T-cell antigen receptor. Science 257:795–797.

Cook WJ, Jeffrey LC, Sullivan MI, Vierstra RD (1992) Three-dimensional structure of a ubiquitin-conjugating enzyme (E2). J Biol Chem 267:15116–15121.

Cox EC, Muller B, Bonhoeffer F (1990) Axonal guidance in the chick visual system: posterior tectal membranes induce collapse of growth cones from the temporal retina. Neuron 4:31–37.

Davies JA, Cook GMW, Stern CD, Keynes RJ (1990) Isolation from chick somites of a glycoprotein fraction that causes collapse of dorsal root ganglion growth cones. Neuron 4:11–20.

Dodd J, Jessell TM (1988) Axon guidance and the patterning of neuronal projections in vertebrates. Science 242:692–699.

Dodd J, Morton SB, Karagogeos D, Yamamoto M, Jessell TM (1988) Spatial regulation of axonal glycoprotein expression on subsets of embryonic spinal neurons. Neuron 1:105–116.

Doherty P, Ashton SV, Moore SE, Walsh FS (1991) Morphoregulatory activities of NCAM and N-cadherin can be accounted for by G protein-dependent activation of L- and N-type neuronal Ca^{+2} channels. Cell 67:21–33.

Edgecomb RS, Ghetti C, Schneiderman AM (1993) *bendless* alters thoracic musculature in *Drosophila*. J Neurogenet 8:201–219.

Ellison KS, Gwozd T, Prendergast JA, Paterson MC, Ellison MJ (1991) A site-directed approach for constructing temperature-sensitive ubiquitin-conjugating enzymes reveals a cell cycle function and growth function for RAD6. J Biol Chem 266:24116–24120.

Faissner A, Kruse J (1990) J1/tenascin is a repulsive substrate for central nervous system neurons. Neuron 5:627–637.

Gao WQ, Liu XL, Hatten ME (1992) The *weaver* gene encodes a nonautonomous signal for CNS neuronal differentiation. Cell 68:841–854.

Glotzer M, Murray AW, Kirschner MW (1991) Cyclin is degraded by the ubiquitin pathway. Nature 349:132–138.

Grenningloh G, Bieber AJ, Rehm EJ, Snow PM, Traguina ZR, Hortsch M, Patel NH, Goodman CS (1990) Molecular genetics of neuronal recognition in *Drosophila*: evolution and function of immunoglobulin superfamily cell adhesion molecules. Cold Spring Harbor Symp Quant Biol 55:327–340.

Grenningloh G, Rehm EJ, Goodman CS (1991) Genetic analysis of growth cone guidance in *Drosophila*: fasciclin II functions as a neuronal recognition molecule. Cell 67:45–57.

Guan KL, Deschenes RJ, Dixon JE (1992) Isolation and characterization of a second protein tyrosine phosphatase gene, PTP2, from *Saccharomyces cerevisae*. J Biol Chem 267:10024–10030.

Herschko A (1991) The ubiquitin pathway for protein degradation. Trends Biochem Sci 16:265–268.

Hochstrasser M (1992) Ubiquitin and intracellular protein degradation. Curr Opin Cell Biol 4:1024–1031.

Hondermarck H, Sy J, Bradshaw RA, Arfin SM (1992) Dipeptide inhibitors of ubiquitin-mediated protein turnover prevent growth factor-induced neurite outgrowth in rat pheochromocytoma PC12 cells. Biochem Biophys Res Commun 189:280–288.

Hotta Y, Benzer S (1972) Mapping behaviour in *Drosophila* mosaics. Nature 240:152–160.

Hynes RO (1992) Integrins: versatility, modulation, and signaling in cell adhesion. Cell 69:11–25.

Hynes RO, Lander AD (1992) Contact and adhesive specificities in the associations, migrations and targeting of cells and axons. Cell 68: 303–322.

Jay DG, Keshishian H (1990) Laser inactivation of fasciclin I disrupts axon adhesion of grasshopper pioneer neurons. Nature 348:548–550.

Jentsch S (1992) The ubiquitin-conjugation system. Annu Rev Genet 26:179–207.

Jentsch S, McGrath JP, Varchavsky A (1987) The DNA repair gene RAD6 encodes a ubiquitin-conjugating enzyme. Nature 329:131–134.

Kankel DR, Hall JC (1976) Fate mapping of nervous system and other internal tissues in genetic mosaics of *Drosophila melanogaster*. Dev Biol 48:1–24.

Kapfhammer JP, Raper JA (1987) Collapse of growth cone structure on contact with specific neurites in culture. J Neurosci 7:201–212.

Kater SB, Guthrie PB (1990) Neuronal growth cone as an integrator of complex environmental information. Cold Spring Harbor Symp Quant Biol 55:359–370.

Keynes R, Cook G (1990) Cell–cell repulsion: clues from the growth cone? Cell 62:609–610.

King DG, Tanouye MA (1983) Anatomy of motor axons to direct flight muscles in *Drosophila*. J Exp Biol 105:231–239.

King DG, Wyman RJ (1980) Anatomy of the giant fiber pathway in *Drosophila*. I. Three thoracic components of the pathway. J Neurophysiol 9:753–770.

Koken M, Reynolds P, Bootsma D, Hoeijmakers J, Prakash S, Prakash L (1991a) Dhr6, a *Drosophila* homolog of the yeast DNA-repair gene RAD6. Proc Natl Acad Sci USA 88:3832–3836.

Koken MHM, Reynolds P, Jaspers-Dekker I, Prakash L, Prakash S, Bootsma D, Hoeijmakers JHJ (1991b) Structural and functional conservation of two human homologs of the yeast DNA repair gene RAD6. Proc Natl Acad Sci USA 88:8865–8869.

Kolman CJ, Toth J, Gonda DK (1992) Identification of a portable determinant of cell cycle function within the carboxyl-terminal domain of the yeast CDC34 (UBC3) ubiquitin-conjugating (E2) enzyme. EMBO J 11:3081–3090.

Koto M (1983) Morphology of giant fiber system neurons in wild-type and mutant *Drosophila melanogaster*. PhD thesis, Yale University.

Koto M, Tanouye MA, Ferrus A, Thomas JB, Wyman R (1981) The morphology of the cervical giant fiber neuron of *Drosophila*. Brain Res 221:213–217.

Krishnan SN, Frei E, Swain GP, Wyman RJ (1983) Passover: a gene required for synaptic connectivity in the giant fiber system of *Drosophila*. Cell 73:967–977.

Laszlo L, Doherty FJ, Osborn NU, Mayer RJ (1990) Ubiquitinated protein conjugates are specifically enriched in the lysosomal system of fibroblasts. FEBS Lett 261:365–368.

Lindsley DL, Zimm GG (1992) The genome of *Drosophila* melanogaster. San Diego: Academic.

Lohof AM, Quillan M, Dan Y, Poo M (1992) Asymmetric modulation of cytosolic cAMP activity induces growth cone turning. J Neurosci 12:1253–1261.

McIntire SL, Garriga G, White J, Jacobson D, Horvitz HR (1992) Genes necessary for directed axonal elongation or fasciculation in *C. elegans*. Neuron 8:307–322.

Meyerowitz EM, Kankel DR (1978) A genetic analysis of visual system development in *Drosophila melanogaster*. Dev Biol 62:112–142.

Morganti MC, Taylor J, Pesheva P, Schachner M (1990) Oligodendrocyte-derived J1-160/180 extracellular matrix glycoproteins are adhesive or repulsive depending on the partner cell type and time of interaction. Exp Neurol 109:98–110.

Mori S, Heldin C-H, Claesson-Welsh L (1992) Ligand-induced polyubiquitination of the platelet-derived growth factor β-receptor. J Biol Chem 267:6429–6434.

Muralidhar MG, Thomas JB (1993) The *Drosophila bendless* gene encodes a neural protein related to ubiquitin-conjugating enzymes. Neuron 11:253–266.

Murti KG, Smith HT, Fried VA (1988) Ubiquitin is a component of the microtubule network. Proc Natl Acad Sci USA 85:3019–3023.

Nose A, Mahajan VB, Goodman CS (1992) Connectin: a homophilic cell adhesion molecule expressed on a subset of muscles and the motorneurons that innervate them in *Drosophila*. Cell 70:553–567.

Okamato H, Kuwada JY (1991) Alteration of pectoral fin nerves following ablation of fin buds and by ectopic fin buds in the Japanese Medaka fish. Dev Biol 146:62–71.

O'Rourke AM, Mescher MF (1992) Cytotoxic T lymphocyte activation involves a cascade of signaling and adhesion events. Nature 358: 253–255.

O'Rourke NA, Fraser SE (1990) Dynamic changes in optic fiber terminal arbors lead to retinotopic map formation: an *in vivo* confocal microscopic study. Neuron 5:159–171.

Ota IM, Varshavsky A (1992) A gene encoding a putative tyrosine phosphatase suppresses lethality of an N-end rule-dependent mutant. Proc Natl Acad Sci USA 89:2355–2359.

Paolini R, Kinet J-P (1993) Cell surface control of the multiubiquitination and deubiquitination of high-affinity immunoglobulin E receptors. EMBO J 12:779–786.

Patterson PH (1988) On the importance of being inhibited, or saying no to growth cones. Neuron 1:263–267.

Pearson WR, Lipman DJ (1988) Improved tools for biological sequence comparison. Proc Natl Acad Sci USA 85:2444–2448.

Pesheva P, Gennaarini G, Goridis C, Schachner M (1993) The F3/11 cell adhesion molecule mediates the repulsion of neurons by the extracellular matrix glycoprotein J1-160/180. Neuron 10:69–82.

Phillips DR, Charo IF, Scarborough RM (1991) GPIIb-IIIa: the responsive integrin. Cell 65:359–362.

Phillis RW, Bramlage AT, Wotus C, Whittake A, Gramates LS, Seppala D, Farahanchi F, Caruccio P, Murphey RK (1993) Isolation of mutations affecting neural circuitry required for grooming behavior in *Drosophila melanogaster*. Genetics 133:581–592.

Poole SJ, Kauvar LM, Drees B, Kornberg T (1985) The engrailed locus of *Drosophila*: structural analysis of an embryonic transcript. Cell 40:37–43.

Ready DF, Hanson TE, Benzer S (1976) Development of the *Drosophila* retina, a neurocrystalline lattice. Dev Biol 53:217–240.

Rechsteiner M (1991) Natural substrates of the ubiquitin proteolytic pathway. Cell 66:615–618.

Roberts JD (1986) *Drosophila*: a practical approach. Oxford: IRL.

Sambrook J, Fritsch EF, Maniatis T (1989) Molecular cloning: a laboratory manual. Cold Spring Harbor, NY: Cold Spring Harbor Laboratory.

Schweighoffer T, Shaw S (1992) Adhesion cascades: diversity through combinatorial strategies. Curr Opin Cell Biol 4:824–829.

Seeger M, Tear G, Ferres-Marco D, Goodman CS (1993) Mutations affecting growth cone guidance in *Drosophila*: genes necessary for guidance toward or away from the midline. Neuron 10:409–426.

Selleck SB, Steller H (1991) The influence of retinal innervation on neurogenesis in the first optic ganglion of *Drosophila*. Neuron 6:83–99.

Seufert W, Jentsch S (1990) Ubiquitin-conjugating enzymes UBC4 and UBC5 mediate selective degradation of short-lived and abnormal proteins. EMBO J 9:543–550.

Sharon G, Raboy B, Parag HA, Dimitrovsky D, Kulka RG (1991) RAD6 gene product of *Saccharomyces cerevisiae* requires a putative ubiquitin protein ligase (E3) for the ubiquitination of certain proteins. J Biol Chem 266:15890–15894.

Smith SJ (1988) Neuronal cytomechanics: the actin based motility of growth cones. Science 242:708–715.

Steller H, Fischbach KF, Rubin GM (1987) *disconnected*: a locus required for neuronal pathway formation in the visual system of *Drosophila*. Cell 50:1139–1153.

Strathman M, Hamilton BA, Mayeda CA, Simon MI, Meyerowitz EM, Palazzolo MP (1991) Transposon-facilitated DNA sequencing. Proc Natl Acad Sci USA 88:1247–1250.

Sullivan ML, Vierstra RD (1991) Cloning of a 16 kDa ubiquitin carrier protein from wheat and *Arabidopsis thaliana*: identification of functional domains by *in vitro* mutagenesis. J Biol Chem 266:23878–23885.

Tanaka E, Kirschner M (1991) Microtubule behavior in the growth cones of living neurons during axon elongation. J Cell Biol 115:345–363.

Tanouye MA, King DG (1983) Giant fiber activation of direct flight muscles in *Drosophila*. J Exp Biol 105:241–251.

Tanouye MA, Wyman RJ (1980) Motor outputs of giant nerve fiber in *Drosophila*. J Neurophysiol 44:405–421.

Tessier-Lavigne M (1992) Axon guidance by molecular gradients. Curr Opin Neurobiol 2:60–65.

Tessier-Lavigne M, Placzek M, Lumsden AGS, Dodd J, Jessell TM (1988) Chemotropic guidance of developing axons in the mammalian nervous system. Nature 336:775–778.

Thomas JB, Wyman RJ (1982) A mutation in *Drosophila* alters normal connectivity between two identified neurons. Nature 298:650–651.

Thomas JB, Wyman RJ (1984) Mutations altering synaptic connectivity between identified neurons in *Drosophila*. J Neurosci 4:530–538.

Treier M, Seufert W, Jentsch S (1992) *Drosophila* UbcD1 encodes a highly conserved ubiquitin-conjugating enzyme involved in selective protein degradation. EMBO J 11:367–372.

Trimarchi JR, Schneiderman AM (1993) Giant fiber activation of an intrinsic muscle in the mesothoracic leg of *Drosophila melanogaster*. J Exp Biol 177:149–167.

van der Bliek AM, Meyerowitz EM (1991) Dynamin-like protein encoded by the *Drosophila shibire* gene is associated with vesicular traffic. Nature 351:411–414.

Vihtelic TS, Hyde D, O'Tousa JE (1991) Isolation and characterization of the *Drosophila retinal degeneration B* (*rdgB*) gene. Genetics 127: 761–768.

Walter J, Allsopp TE, Bonhoeffer F (1990) A common denominator of growth cone guidance and collapse. Trends Neurosci 13:447–452.

Wiebel F, Kunau WH (1992) The Pas2 protein essential for peroxisome biogenesis is related to ubiquitin-conjugating enzymes. Nature 359:73–76.

Wyman R, Thomas JB (1983) What genes are necessary to make an identified synapse? Cold Spring Harbor Symp Quant Biol 48:641–652.

Wyman RJ, Thomas JB, Salkoff L, King DG (1984) The *Drosophila* giant fiber system. In: Neural mechanisms of startle behavior (Eaton R, ed), pp 133–166. New York: Plenum.

Yarden Y, Escobedo JA, Kuang W-J, Yang-Feng TL, Daniel TO, Tremble PM, Chen EY, Ando ME, Harkins RN, Francke U (1986) Structure of the receptor for platelet-derived growth factor helps define a family of closely related growth factor receptors. Nature 323:226–232.

Zipursky SL, Venkatesh TR, Teplow DB, Benzer S (1984) Neuronal development in the *Drosophila* retina: monoclonal antibodies as molecular probes. Cell 36:15–26.